

FEDSM2003-45207

IMPROVED SNR BY COMBINING ENSEMBLE AVERAGING AND ZERO-ORDER CORRELATION

D. P. Hart

Massachusetts Institute of Technology
Cambridge, MA 02129

C. Meinhart

University of Santa Barbara
Santa Barbara, CA

ABSTRACT

This paper presents a technique for improving the signal-to-noise ratio of microPIV data. The technique marries the advantages of ensemble averaging [Meinhart, '00] and Correlation Based Correction, CBC [Hart, '99].

Multiplying, element-by-element, the correlation coefficients obtained over time from an interrogation region results in high noise rejection greatly improving the correlation signal-to-noise ratio. However, in the case where particle density is relatively low, a single correlation function may or may not contain a signal peak. If a correlation function is included in the temporal sequence that does not contain a signal peak, the signal from the entire correlation sequence is lost. This problem is avoided by ensemble averaging correlation planes in time rather than multiplying them element-by-element. Ensemble averaging increases signal by increasing the effective particle density of the flow, without increasing the particle loading in the fluid. However, when using only the ensemble averaging technique, one may need to average hundreds of images to obtain high signal to noise.

INTRODUCTION

The purpose of all PIV image processing algorithms is to obtain accurate velocity data while minimizing the number of spurious vectors. It is often desirable to decrease interrogation cell size to improve spatial resolution. For high shearing flows, decreasing cell size can improve signal quality by minimizing the velocity gradient across the cell. However, decreasing the cell size can also have negative effects. It can decrease accuracy of the velocity measurement, and it can increase the number of spurious vectors. In some cases, this problem can be reduced by simply increasing the seeding density. In other cases, such as microPIV, seeding density must be kept sufficiently low in order to maintain visibility of in-focus particle images.

Improvements in signal to noise and spatial resolution of the velocity measurements can be obtained by ensemble averaging a time series of correlation functions together

[Meinhart et al. '00; Westerweel]. By ensemble averaging correlation functions obtained from a set of 20 image data fields, Meinhart et al. [99] obtained temporal-averaged velocity data with a spatial resolution of $0.9 \mu\text{m} \times 13.8 \mu\text{m} \times 1.8 \mu\text{m}$ in a microchannel.

Ensemble averaging correlation data increases signal to noise linearly with the number of averages. The signal to noise can also be increased by multiplying the time series of correlation functions together instead of adding them. This was demonstrated by Hart [98].

Here, the authors present a PIV processing algorithm, where the techniques of adding and multiplying correlation functions are combined. The correlation tables from an interrogation region are ensemble averaged in time over different intervals. The averaged correlation tables are then multiplied element-by-element. This greatly reduces the noise levels in the correlation domain. By averaging the correlation tables before multiplying them, the likelihood of having a data set with no correlation information is reduced.

In this paper, the authors investigate the manner in which this approach is best implemented – seeking the optimum number of correlation planes to average before multiplying to achieve the greatest signal-to-noise ratio from a minimal number of images. The optimum sequence is thought to depend upon the particle image density, and the signal to noise ratio in the particle-image field.

NOMENCLATURE

a	object plane location
d_p	particle diameter
f	f-number
m	geometric averaging number
n	arithmetical averaging number, particle density, index of refraction
r	particle radius
s_o	object distance

x	coordinate
y	coordinate
z_0	focal length
z_{corr}	measurement domain thickness
C	particle concentration
D	aperture diameter
F	fill ratio
I	image intensity
L	test section thickness
M	magnification
N	interrogation size (pixels)
N	total averaging number
NA	numerical aperture
R	correlation function
V	particle visibility, interrogation volume
λ	wavelength of light
Δ	particle separation
ϕ	correlation function
Γ	signal gain factor

Correlation Noise

Correlation *noise* (signal within the correlation table that does not represent the primary correlation peak) is, in general, the cause of peak locking and spurious vector generation. In order to understand the source of correlation noise, consider the signal obtained from the correlation of a single tracer particle pair.

Due to optical diffraction, images of tracer particles appear roughly Gaussian with a radius equal to $\sqrt{M^2 d_p^2 + (2.44 \cdot \frac{\lambda \cdot z_0}{D})^2}$ where d_p is the diameter of the tracer particles, M is the image magnification, and λ is the wavelength of the imaged light, z_0 is the focal length of the imaging optics, and D is the aperture diameter. The direct correlation of two particle images neglecting image discretization effects can be estimated in terms of particle separation distance Δ ;

$$\Phi = \int_{-\infty}^{\infty} \int_{-\infty}^{\infty} I^2 e^{-\frac{x^2+y^2}{r^2}} e^{-\frac{(x-\Delta)^2+y^2}{r^2}} dx dy = \frac{\pi r^2 I^2}{2} e^{-\frac{\Delta^2}{2r^2}} \quad (1)$$

where r is the radius of the particle image and I is the peak intensity of the particle image. The resulting correlation profile is also approximately Gaussian but with a radius of $\sqrt{2}r$ rather than r and a magnitude that is a function of r^2 , Fig. 1.

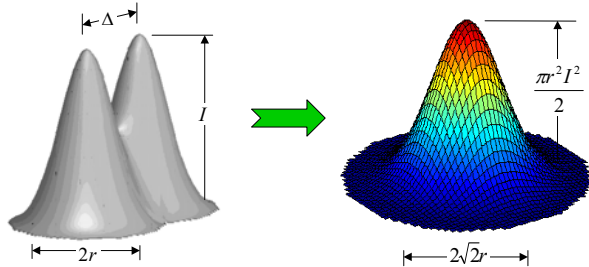


Figure 1. - The correlation of two tracer particle image pairs of radius r yields a correlation peak that is Gaussian with a radius of $\sqrt{2}r$ and magnitude that is a function of r^2 .

Correlation Noise at Low Seeding Density

At very low seeding densities (image density less than about 10%), the probability of the overlap of more than one particle image for any given correlation window offset is relatively small. Consequently, on average, the magnitude of the *correlation noise* at low seeding densities is equal to the correlation of a single pair of particle images, $\frac{\pi r^2 I^2}{2}$. The magnitude of the *correlation signal*, however, is roughly equal to the number of particles in the interrogation region, n , times the magnitude of the correlation of a single particle pair, $\frac{n\pi r^2 I^2}{2}$. Therefore, at low seeding densities, the correlation signal-to-noise ratio scales approximately as the number of particles, $SNR \cong n$, Fig. 2.

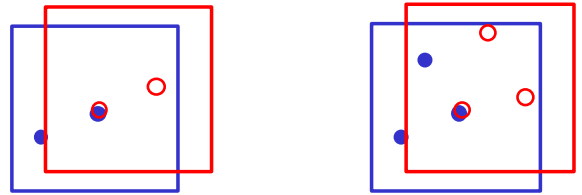


Figure 2. - At low seeding densities when the number of tracer particle images per interrogation region is small, on average, only one particle image pair aligns at a time. Consequently, the correlation signal-to-noise ratio scales as the number of particles, $SNR \cong n$.

Correlation Noise at High Seeding Density

At high seeding densities, more than one particle image typically overlaps at each window offset, Fig. 3. Consequently, at high seeding densities, the level of correlation noise increases with seeding density since the average particle image overlap increases with seeding density. Consider any two adjacent tracer particle images within an interrogation region, Fig. 4.

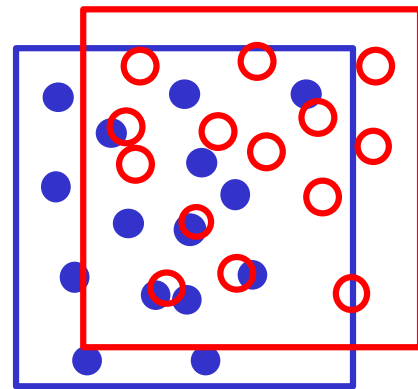


Figure 3. - At high seeding densities, more than one particle image overlaps at any window offset. The result is an increase in the relative correlation noise level compared with the peak correlation.

$$\text{Particle Spacing} \sim \frac{N}{\sqrt{n}}$$

Figure 4. - The spacing between adjacent particle images within an interrogation region is proportional to N/\sqrt{n} .

If these tracer particle images exist within an $N \times N$ region, then, from dimensional analysis, one would expect that the average spacing between any two particle images would be a function of N/\sqrt{n} . The average correlation noise can thus, be determined by calculating the mean correlation strength based on a uniform distribution of particle spacing centered on a spacing that is a function of N/\sqrt{n} . Using the results for an individual particle correlation, Eq. 1, the average correlation noise can be determined based on a single coefficient, k ;

$$\begin{aligned} & \frac{n\sqrt{n}}{Nk} \int_0^{\frac{Nk}{\sqrt{n}}} e^{-\frac{\Delta^2}{2r^2}} d\Delta \\ &= \frac{n\sqrt{2}}{2k} \sqrt{\frac{n\pi r^2}{N^2}} \operatorname{erf}\left(k \frac{\sqrt{2\pi}}{2} \sqrt{\frac{N^2}{n\pi r^2}}\right) \end{aligned} \quad (2)$$

where $k = \sqrt{\frac{2}{\pi}}$ if a normal distribution of particles within the interrogation region is assumed. Therefore, the correlation signal-to-noise ratio at high seeding densities is equal to,

$$SNR \cong 1 / \left(\frac{\sqrt{F\pi}}{2} \operatorname{erf}\left(\frac{1}{\sqrt{F}}\right) \right) \quad (3)$$

$$\text{where } F \equiv \text{Fill Ratio (Image Density)} = \frac{n\pi r^2}{N^2}.$$

The total signal strength, $1-1/SNR$, can be approximated by adding the SNR components due to individual particle correlations and correlations of particle overlap,

$$1 - 1/SNR \cong 1 - \frac{1}{2} \sqrt{F\pi} - \frac{1}{n}. \quad (4)$$

Figure 5 illustrates the relative signal strength due to individual particle correlations and particle overlap. At low fill ratios, the SNR is a direct function of the number of particles within an interrogation region. At high fill ratios, the SNR is almost entirely influenced by the fill ratio rather than the number of particles.

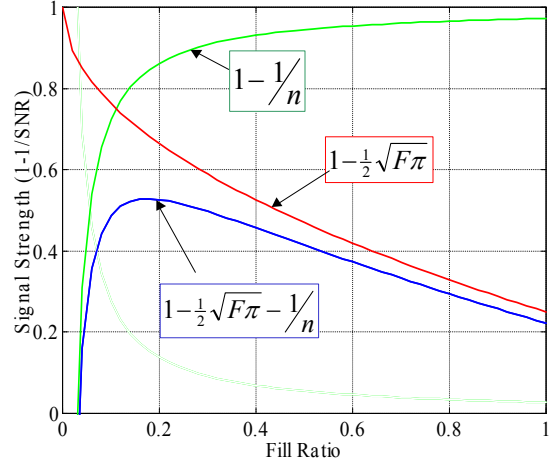


Figure 5. - Relative signal strength, $1-1/SNR$, as a function of the image fill ratio. At low fill ratios, the signal strength is a direct function of the number of particles within the interrogation region, n . At high seeding densities, the signal strength is dominated by the fill ratio, F .

Figure 6 illustrates the accuracy to which Eq. 4 predicts the signal strength. Here, the correlation signal strength calculated from synthetic data for two different interrogation areas and two different tracer particle image radii is plotted as a function of the fill ratio and compared to Eq. 4. As is evident in this figure, Eq. 4 does a fair job of predicting the signal strength.

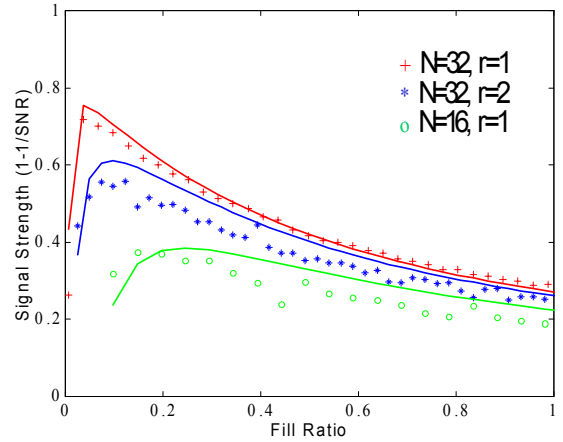


Figure 6. - The signal strength calculated from Eq. 4 (solid lines) is compared with correlation data taken from synthetic images for $N=16$ and 32 , and $r=1$ and 2 . Eq. 4 is relatively accurate in predicting the correlation signal strength.

From this analysis, it is apparent that there exists an optimum seeding density to maximize the correlation SNR. Not surprisingly, the optimum seeding density increases as the interrogation size decreases. This is generally not a problem as one is usually free to increase the number of tracers within a flow to approach this optimum condition without effecting flow characteristics. In ultra-high resolution PIV, flow analysis where small interrogation volumes are used and in micro-PIV systems where out of focus tracer particles degrade image quality, seeding density is severely limited. In these cases, an alternate approach is needed to improve the correlation signal-

to-noise ratio. Herein we focus on improving the SNR in micro-PIV applications but similar arguments can be made for high resolution PIV of time-invariant flows.

VISIBILITY CONSTRAINTS IN MICRO-PIV

Micron resolution particle image velocimetry (micro-PIV) differs from traditional PIV in several aspects, including both particle image acquisition and processing. Image acquisition in micro-PIV is characterized most commonly by using high magnification high numerical aperture lenses to record fluorescently-labeled sub-micron particles. In traditional PIV, the two-dimensional measurement plane is defined by the illuminating light sheet. The small length scale associated with micro-PIV precludes using a light sheet to illuminate a plane of flow-tracing particles. Instead, particles are commonly illuminated through volume illumination using epi-fluorescence imaging [Santiago et al., '98; Meinhart et al. '99].

Figure 7 shows the characteristic geometry of an epi-fluorescence illumination system. The measurement domain has thickness z_{corr} and is related to the depth of field of the objective lens. Several theories have been proposed to estimate measurement domain thickness, see Olsen & Adrian ['00] and Meinhart et al. ['00].

Olsen & Adrian ['00] present a theory to predict particle visibility for micro-PIV systems. This theory can be used to estimate maximum particle concentrations for specific experimental parameters: particle size, test section thickness, and objective lens f -number. For infinity-corrected objective lenses, the f -number can be approximately related to the numerical aperture $f^{\#} \approx 1/2 \left[(n/NA)^2 - 1 \right]^{1/2}$ [Meinhart & Wereley, '03]. Where n is the index of the recording medium, and NA is the numerical aperture of the recording lens. Writing the in-focus particle visibility, V , developed by Olsen & Adrian ['00] in terms of numerical aperture, and rearranging, one can estimate maximum particle concentration, C , that can be used while maintaining a sufficient particle visibility.

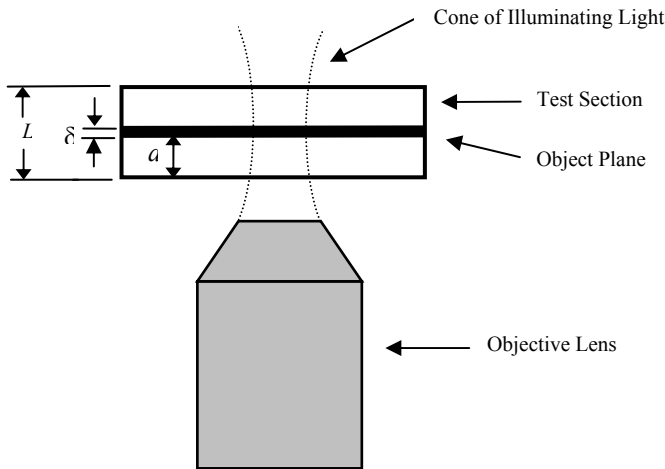


Figure 7. Schematic showing the geometry for volume illumination particle image velocimetry. Particles located within the plane of thickness δ are considered to be well focused and contribute to velocity signal. Particles outside this region are considered to be out of focus and contribute to background noise.

$$C = \frac{4\beta^2 (s_o - a)(s_o - a + L)}{\pi V L s_o^2 \left[d_p^2 + 1.49\lambda^2 \left(\left(\frac{n}{NA} \right)^2 - 1 \right) \right]} \quad (5)$$

The maximum concentration is dependent upon the object distance of the recording lens, s_o , the imaging distance inside the test section, a , the wavelength of light, λ , and particle diameter, d_p . The constant β is usually chosen to be $\beta^2 = 3.67$. Equation (5) shows the strong relationship between particle visibility and test section thickness, L . When designing micro-PIV experiments, the thickness of the test section limits the maximum particle concentration that can be used to obtain reliable data. For this reason, high spatial resolution measurements can be more easily obtained using thinner test sections. Meinhart et al. (1999) obtained an in-plane spatial resolution of $0.9 \times 13.8 \times 2 \mu\text{m}$ using an $L = 30 \mu\text{m}$ thick channel.

Let's assume that a visibility, $V = 3$, is sufficient to obtain high quality particle image fields. Table 1 shows the maximum particle concentration that can be used while maintaining $V = 3$, for several common objective lenses, when imaging in the center of an $L = 100 \mu\text{m}$ thick test section.

Table 1. Maximum particle concentration [μm^{-3}] that will allow an in-focus visibility, $V = 3$, for imaging the center of an $L = 100 \mu\text{m}$ deep test section.

Particle Size d_p μm	Microscope Objective Lens Characteristics				
	$M = 60$ $NA = 1.4$ $s_o = 0.38$ mm	$M = 40$ $NA = 0.75$ $s_o = 0.89$ mm	$M = 40$ $NA = 0.6$ $s_o = 3$ mm	$M = 20$ $NA = 0.5$ $s_o = 7$ mm	$M = 10$ $NA = 0.25$ $s_o = 10.5$ mm
0.01	1.9E-1	4.3E-2	1.9E-2	1.1E-2	2.2E-3
0.10	1.7E-1	4.2E-2	1.9E-2	1.1E-2	2.2E-3
0.20	1.3E-1	3.9E-2	1.8E-2	1.1E-2	2.2E-3
0.30	9.0E-2	3.4E-2	1.7E-2	1.1E-2	2.2E-3
0.50	4.6E-2	2.5E-2	1.4E-2	9.4E-3	2.2E-3
0.70	2.7E-2	1.8E-2	1.2E-2	8.2E-3	2.1E-3
1.00	1.4E-2	1.1E-2	8.5E-3	6.5E-3	2.0E-3
3.00	1.7E-3	1.7E-3	1.6E-3	1.5E-3	9.7E-4

Double pulsed cross correlation typically requires $\sim 3 - 5$ particle image pairs to obtain reliable velocity measurements [see Keane & Adrian '90, '92]. Previously published interrogation volumes of micro-PIV measurements range from high resolutions of, say, $0.9 \times 13.8 \times 2 \mu\text{m} = 25 \mu\text{m}^3$ to lower resolutions of, say, $10 \times 10 \times 20 \mu\text{m} = 2000 \mu\text{m}^3$. Assuming that five particle image pairs are required per interrogation spot to obtain reliable velocity data, the require effective particle concentrations would be $2.0\text{E}-1 \mu\text{m}^{-3}$ and $2.5 \text{E}-3 \mu\text{m}^{-3}$ for the high and low resolution cases, respectively.

If the high resolution measurements are taken with an $M = 60$, $NA = 1.4$ oil-immersion lens, using flow-tracing particles of

therefore may not contribute to signal. The probability of finding at least two particles in an interrogation volume is

$$P(k \geq 2) = 1 - P(0) - P(1) = 1 - (1 + CV)e^{-CV}. \quad (8)$$

This probability can be increased by increasing the particle concentration, C , or by increasing the volume of the interrogation region, V . In many situations it may not be practical to increase particle concentration because it may raise the particle volume fraction to unacceptable levels, or in the micro-PIV mode, particle visibility may be reduced to unacceptable levels, see Eq. (5). In addition, it may be undesirable to increase V , because it will reduce the spatial resolution of the measurements. An alternative solution is to add a series of n correlation functions, thereby increasing the probability of finding at least two particles in the series, such that

$$P_n(k \geq 2) = 1 - (1 + nCV)e^{-nCV}. \quad (9)$$

The probability that all of the m multiplicative groups of correlations functions contain at least two particles is

$$P_n^m(k \geq 2) = [1 - (1 + nCV)e^{-nCV}]^m. \quad (10)$$

If at least two particles are required in each multiplicative group to obtain a reliable measurement, then Eq. (10) is an estimate of the probability of obtaining reliable velocity measurements. The parameters n and m must be judiciously chosen such that P_n^m is sufficiently large, say $P_n^m \sim 0.98$, so that 98% of the data is reliable.

The probabilities for successful measurements estimated by Eq. (10) are shown in Figure 9, for $N = 10, 20$ and 100 . There exists a sharp cutoff in the predicted success rate of the measurements with decreasing seeding density. When particle seeding densities are low, it is important to use as many correlation functions as possible, and to emphasize arithmetic averaging, such that $n \approx N$ or $N/2$ and $m \approx 1$ or 2 .

Let's consider a marginal seeding density case, where on average there is one particle per interrogation volume, $CV = 1$. If the number of correlation functions is limited to $N = 10$, then only the arithmetic average can be used, i.e. $n = 10, m = 1$. Extending the number of correlation functions to $N = 20$ provides enough sample so that one multiplication can be performed, $n = 10, m = 2$, without loss of signal. Further extending the number of correlations to $N = 100$, allows us to perform the same number of multiplications as additions, where $n = 10, m = 10$.

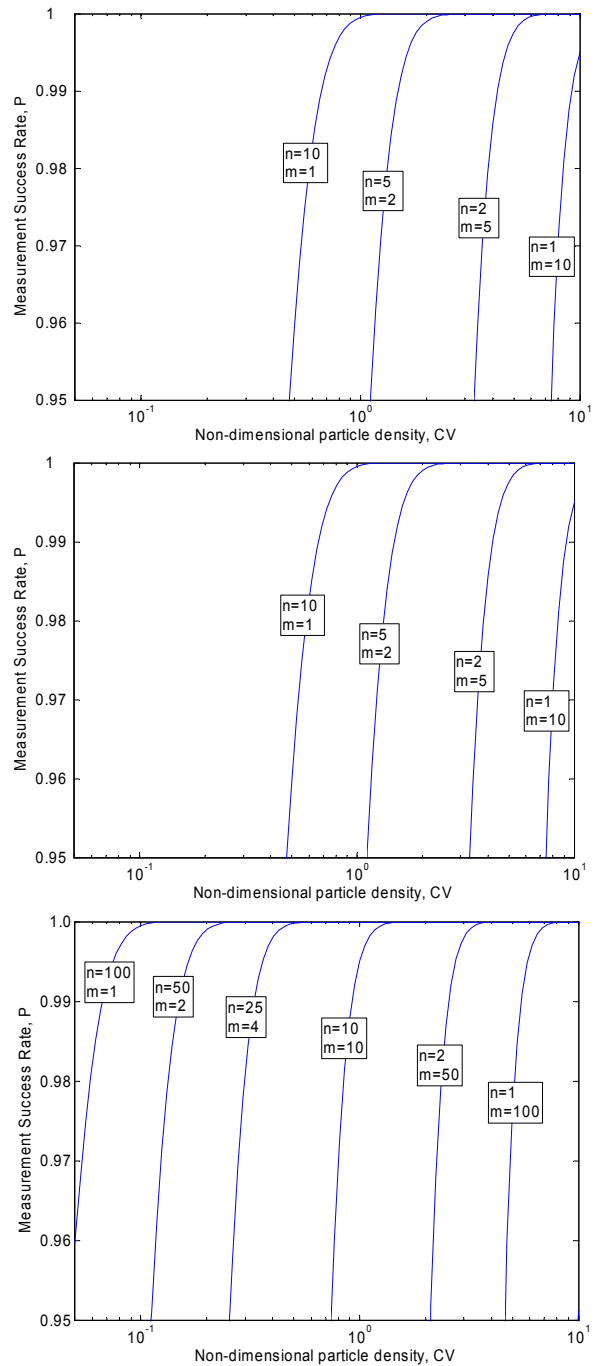


Figure 9. Probability of obtaining a reliable velocity measurement, $P_n^m(k \geq 2)$ from Eq. (6). Here we use the criterion that at least two particles must be present to contribute to the correlation signal peak. The total number of correlation functions, N , used in the calculation are: (a) $N = 10$, (b) $N = 20$ and (c) $N = 100$.

SPATIAL RESOLUTION VS. SIGNAL STRENGTH

Fig. 9c shows that a large number of correlations allows one to obtain measurements with very low particle concentrations. With $n = 100, m = 1$, particle concentrations approaching $CV = 0.005$ can produce approximately 96%

reliable vectors. This feature is often exploited in micro-PIV where low particle concentrations are necessary to maintain adequate particle visibility while achieving high spatial resolution. It is evident from Fig. 9 that multiplying correlation functions will probably not be effective for improving spatial resolution, compared to just arithmetically averaging the correlation functions. When particle concentration is sufficiently high to obtain reliable measurements, then multiplying the correlation functions will drastically increase signal strength, thereby improving the quality of the signal.

REFERENCES

- Adrian RJ (1991) Particle-imaging techniques for experimental fluid mechanics. *Annu. Rev. Fluid Mech*, Vol. 23, pp. 261-304.
- Deen, N.G., J. Westerweel & E. Delnoij. Two-phase PIV in bubbly flows: status and trends. *Chem. Eng. Technol.* 25 (2002) 97-101.
- Delnoij, E., J.A.M. Kuipers, W.P.M. van Swaaij & J. Westerweel. Measurement of gas-liquid two-phase flow in bubble columns using ensemble correlation PIV. *Chem. Eng. Sci.* 55 (2000) 3385-3395.
- Hart, D. P., "PIV Error Correction," *Experiments in Fluids*, 1999.
- Hart, D. P., "Super-Resolution PIV by Recursive Local-Correlation," *Journal of Visualization*, The Visualization Society of Japan, Vol. 10, 1999.
- Keane RD, Adrian RJ (1990) Optimization of particle image velocimeter: I Double pulsed systems. *Meas. Sci. Technol.* 1, 1202-1215.
- Keane RD, Adrian RJ (1992) Theory of cross-correlation analysis of PIV images. *Applied Scientific Research*, 49, 1-27.
- Meinhart CD, Wereley ST & Santiago JG (1999) PIV Measurements of a Microchannel Flow. *Exp. in Fluids*, 27, 414-419.
- Meinhart CD, Wereley ST, Santiago JG (2000), A PIV algorithm for estimating time-averaged velocity fields, *Journal of Fluids Engineering*, 122, 285-289.
- Meinhart CD, Wereley ST (2003) The Theory of Diffraction-Limited Resolution in Micro Particle Image Velocimetry *Meas. Sci. Technol.* (submitted).
- Olsen MG and Adrian RJ (2000) Out-of-focus effects on particle image visibility and correlation in microscopic particle image velocimetry, *Exp. in Fluids*, (Suppl.), S166-S174.
- Raffel, M.; Kompenhans, J., (1994) "Error Analysis for PIV recording Utilizing Image Shifting," *Proc. 7th International Symposium on Applications of Laser Techniques to Fluid Mechanics*, Lisbon, July, p. 35.5.
- Westerweel, J., *Digital Particle Image Velocimetry Theory and Application*. Delft University Press (1993).
- Westerweel, J. (1994) "Efficient Detection of Spurious Vectors in Particle Image Velocimetry Data," *Experiments in Fluids*, Vol. 16, pp. 236-247.
- Westerweel, J.; Dabiri, D.; Gharib, M., (1997) "The Effect of a Discrete Window Offset on the Accuracy of Cross-Correlation Analysis of Digital PIV Recordings," *Experiments in Fluids*, Vol. 23, pp. 20-28.
- Westerweel, J., C. Poelma & R. Lindken Two-point ensemble correlation method for mPIV applications. In: *Proc. 11th Int. Symp. on Applications of Laser Techniques to Fluid Mechanics* (Lisbon, Portugal) July 8-11, 2002.
- Willert, C. E.; Gharib, M. (1991) "Digital Particle Image Velocimetry," *Experiments in Fluids*, Vol. 10, pp. 181-193.